

Latent Policy Steering with Embodiment-Agnostic Pretrained World Models

Yiqi Wang¹ and Mrinal Verghese¹ and Jeff Schneider¹

Abstract—The performance of learned robot visuomotor policies is heavily dependent on the size and quality of the training dataset. While an increasing amount of robot or human data is publicly available, embodiment gaps and differing action spaces can make leveraging these data challenging. In this work, we aim to learn visuomotor policies in a low-data regime by pretraining a model across embodiments (e.g., humans and multiple robots). Our approach pretrains a World Model (WM) with embodiment-agnostic action representations based on optical flow on easily-collected or readily available multi-embodiment data. This WM is finetuned on a small dataset collected on the target robot-embodiment (data collection < 1 hour). To leverage this WM, we develop Latent Policy Steering (LPS), a technique that rolls out action candidates and identifies the best action during inference based on a learned value function robust to distribution shifts. In the real-world experiments, our method achieves over 50% relative improvement with 30-50 target-embodiment demonstrations, and over 25% relative improvement with 50-100 demonstrations, compared to a pure imitation learning baseline.

I. INTRODUCTION

Imitation learning through Behavior Cloning (BC) is a widely adopted paradigm to acquire visuomotor policies for robots [1][2][3]. To achieve high task success, sufficient expert demonstrations must be collected, which is a time-consuming process. Furthermore, the data collected are often specific to a robot, a task, or an environment, and the data collection process may need to be repeated for different embodiments or different environments. Thanks to the progress in collecting large datasets [4] across different robots and environments, progress has been made to build generalist robot policies [5][6] via cross-embodiment training. However, these models sometimes do not generalize to new tasks with satisfactory results. To finetune these models for better performance, a considerable amount of data is required, given the large model size used to learn from large datasets [1][3][7]. For example, $\pi 0$ [7] requires 5-10 extra hours of fine-tuning data to achieve high success rates on new tasks.

According to historical Machine Learning research, a model trained on large and diverse datasets across multiple tasks will produce general representations that are transferable to new tasks with only a small amount of data, known as pretraining [6][8]. However, pretraining a robot model is challenging: each robot in the dataset has embodiment-specific information (proprioception, actions). Thus, a pre-training dataset with different embodiments makes the pre-

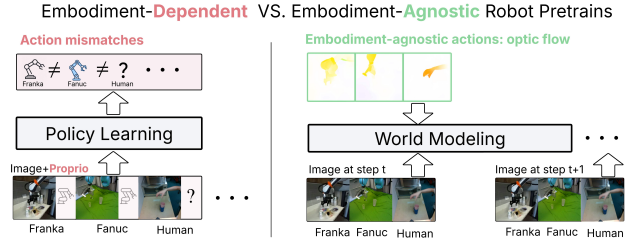


Fig. 1. **World Model (WM) pretraining with optical flow as an embodiment-agnostic action representation.** Thanks to optical flow, we can integrate data from multiple types of embodiments (robots, humans), with a shared action space. A WM is chosen for pretraining since it can leverage suboptimal data. We encode every optical flow to a vector input of the WM, and train the encoder end-to-end with the WM.

trained representation heavily dependent on the embodiments included in the dataset and may generalize poorly to new embodiments.

To tackle this unique challenge, we choose to pretrain a robot World Model (WM) with an embodiment-agnostic action representation: optical flow (Fig. I). Since optical flow captures visual motion in the pixel space, it is less dependent on the specific embodiment and allows different embodiments to share the same action space. Instead of a policy, we choose to pretrain a WM with optical flow because a WM can leverage suboptimal data. During inference, such a WM will improve a policy via policy steering [9], [10], [11] to improve the performance of the policy.

To leverage the pretrained WM, we propose Latent Policy Steering (LPS), a technique to improve a policy with the WM during inference, motivated by prior work on using a WM for planning and control [12][13]. In that work, the authors simulate the action plan sampled from the policy with the WM by predicting future states and comparing them to a goal image in the latent space. Unfortunately, that technique becomes less effective when the task is long-horizon and the desired outcome (goal image) is beyond the reach of the policy and the WM. Our proposed technique is effective regardless of the task horizon by making one key observation: since every demonstration collected for Behavior Cloning is an expert demonstration that accomplishes the task, every state in the demonstration becomes a goal state. Thus, one can distill the goal-state-to-state comparisons conducted during inference into a state-based value function. Such a value function steers a policy close to the dataset (pessimism [14][15][16][17]), and can approximate the results beyond the horizon. Since behavior cloning methods are vulnerable to distribution shifts, we learn a robust value function on both in-distribution and out-of-distribution data. During inference,

*This work was not supported by any organization

¹ Authors are from Robotics Institute, School of Computer Science, Carnegie Mellon University, 5000 Forbes Ave, Pittsburgh, United States yiqi.w2@andrew.cmu.edu

the robust value function steers a policy toward success by visiting states with higher rewards and closer to the dataset distribution.

Our contributions are as follows.

- We propose optical flow as an embodiment-agnostic action representation to pretrain a World Model (WM) across different robots and human embodiments.
- We propose Latent Policy Steering (LPS) to improve the policy during inference with a WM and a robust value function. To avoid distribution shift, we learn the robust value function on in-distribution and out-of-distribution data. During inference, the LPS steers the policy towards states that have higher rewards and are closer to the dataset rather than deviating from them.
- We demonstrate that LPS with a pretrained WM consistently improves the policy’s performance both in simulated and real-world object manipulation tasks. This shows the effectiveness of improving a policy in small data scenarios by pretraining WMs on abundant task-relevant data from other embodiments.

II. RELATED WORKS

A. Robot Learning from Diverse Data

Collecting large amounts of robot data for a specific task can be challenging and time-consuming. A common strategy to overcome this limitation is to leverage data from other sources, including online robot datasets with multiple types of robots and even human videos. Prior works [18][19][20][21] train a visual encoder using both human and robot video data to avoid learning the policy network from scratch. However, the pretrained encoder only provides visual representations instead of directly learning to make decisions. Thus, to learn full policies across multiple robot embodiments, recent works have also looked at learning a single network across multiple robot embodiments by using a modular structure with a common trunk and various heads for different action spaces [5][22]. Another common approach is the vision-language-action model (VLA) approach, where a pretrained vision-language model is finetuned with robot data to act as a robot policy [23][7][24]. However, due to their large size, both these approaches can be expensive to finetune to improve performance on a specific task, and sometimes suffer from slow inference. We compare our approach against a finetuned HPT [22] as a representative example of these types of models.

Human video is also abundant, but can be challenging to use for robot policies as it lacks specific action information. Some works have attempted to overcome this by learning reusable priors or affordances from human video that can then accelerate robot learning [25][26][13]. However, these approaches tend to make specific assumptions about how humans interact with the world, and may not generalize to tasks that don’t fit these assumptions.

B. Policy Steering & Planning with World Models

Recurrent-state-space-based world models (RSSM) have become an increasingly common approach to model envi-

ronment dynamics and transition functions in robotics. Popularized by Hafner et. al [27][28], these models consist of an encoder, which maps visual observations to a latent state representation, a latent transition function which predicts future latent states, and a decoder which is used primarily during training to propagate gradients. Once trained, these world models can be utilized in a variety of ways. One approach is to learn actor and critic models from the same training data to generate action sequences, roll them out over time, and evaluate them with the critic [28]. Another approach is to encode a goal image in the latent space and then use the similarity between planned states and the goal image as a value function to select the best sequence of actions. These action sequences are commonly optimized using gradient-free optimizers like the Cross-Entropy Method (CEM), but gradient-based optimization can also be used [12][13][28].

These approaches are closely related to policy steering, where a value function and optionally a world model are used to refine the output of a base policy [9], [11]. Policy steering has been shown to compensate for failure modes in the base policy [9] or to select actions from the base policy that obey safety constraints [11]. Using a world model allows the robot to steer its policy based not just on the next action, but on a projected series of actions. We build on the ideas from both planning with World Models and Policy Steering by learning a value function to steer actions from a behavior cloned policy towards states within the data distribution, and closer to the task goal.

C. Offline & Inverse Reinforcement Learning

We propose a value function that favors states in the distribution of the training data, which is related to the pessimism used in offline RL [14][15][16][17] and the concept of Inverse RL [29]. In offline RL, a model (e.g., value functions, dynamics models) only has access to the state-action pairs in an offline dataset. Therefore, predictions for state-action pairs outside of the training data distribution could be unreliable. For example, a value function could be overly optimistic when queried with out-of-distribution state-action pairs, leading to extrapolation errors [14].

D. Optical Flow as a Representation in Robotics

Both 2D optical flow and 3D point flow have commonly been used as intermediate representations in robotics. Multiple works have used 3D flow to represent object affordances [30], [31], [32]. These representations transfer well from simulation to real hardware and can be learned from human videos. Other works have predicted 2D optical flow as an action representation [33], [34] or used optical flow to measure similarity between actions across episodes [33], [35]. Rather than using optical flow as a predicted action representation, in this work, we use optical flow as a unified input action representation to our world model to encode actions across diverse embodiments.

III. PRELIMINARIES

We consider robot control in a Partially Observable Markov Decision Process (POMDP) setting, with a latent

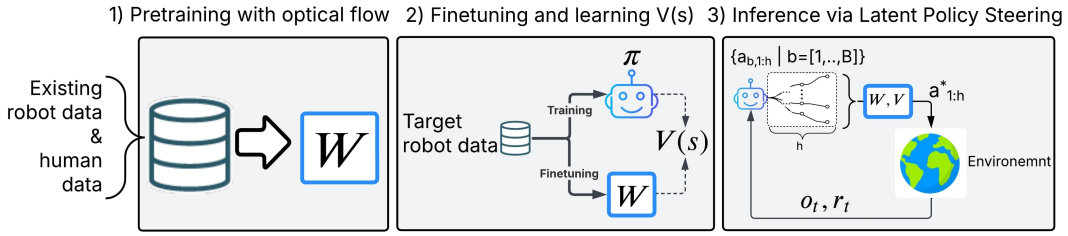


Fig. 2. **Overview of the method.** The figure illustrates all the phases of our method, including WM pretraining, finetuning, and Latent Policy Steering (LPS). After pretraining the WM with optic flow actions, the second phase involves collecting a small robot dataset to learn a policy from scratch, finetuning the WM, and learn a robust value function based on the WM. During inference, the WM and value function are used to select the best candidate.

state space learned by a neural network. A POMDP can be described by a tuple $(\Omega, \mathcal{X}, \mathcal{S}, \mathcal{A}, \mathcal{R}, \mathcal{P})$, which consists of observations $x \in \mathcal{X}$, conditional observation probabilities $\Omega(x'|s, a)$, states $s \in \mathcal{S}$, actions $a \in \mathcal{A}$, reward function $r = \mathcal{R}(s, a)$, and transition function $P(s'|s, a)$. At the timestep $t \in [1, 2, \dots, T]$, the observation, state, action and reward are denoted as o_t, s_t, a_t, r_t . Given discount factor γ , the expected future discounted reward is defined as: $E[\sum_{t=0}^{\infty} \gamma^t r_t]$. A dataset consists of sequences of (x_t, a_t, r_t) where r_t is a binary reward indicating task successes. Given a horizon length h , policy steering seeks the best action plan $\mathbf{a}_t^* = [a_t^*, a_{t+1}^*, \dots, a_{t+h}^*]$ such that: $\mathbf{a}_t^* = \operatorname{argmax}_{a \in \mathcal{A}} \mathbb{E}_{s_t \sim P(\cdot|s_t, a)} \mathcal{R}(s, a)$.

We assume a robot has access to a small dataset of demonstrations for a task on its embodiment (referred to as the target embodiment) and a larger dataset of demonstrations involving similar objects or for a similar task on non-target embodiments, such as other robots or humans.

IV. METHODS

In this section, we first explain our motivation for choosing optical flow as an embodiment-agnostic action representation for pretraining a WM. Then, we describe the proposed technique called Latent Policy Steering (LPS) to leverage a WM to improve the performance of a policy during inference.

A. Flow-as-Action: Embodiment-Agnostic World Modeling

A robot WM that can be easily adapted to a new embodiment should be less dependent on embodiment-specific information during pretraining, such as proprioception and actions. Specifically, to model task dynamics, WMs should use an embodiment-agnostic action representation rather than

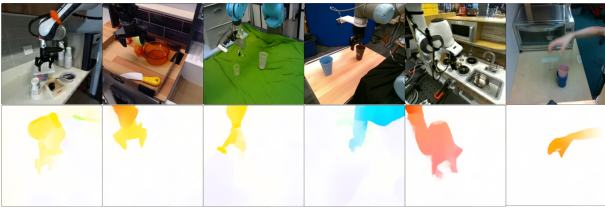


Fig. 3. **Optical flow as an embodiment-agnostic action representation.** We observe that motions captured by optical flow across embodiments are similar in visual space. By using optical flow as an action representation, we remove WM’s dependency on specific embodiments, allowing the pretrained model to efficiently leverage data from multiple embodiments.

a raw robot action as input (embodiment-specific). Unlike prior work, such as HPT [22], which learns generalizable representations on the fly with end-to-end training, we propose to replace the raw action from different embodiments with an existing embodiment-agnostic action representation that is easy to compute with the off-the-shelf tools: optical flow. One of our key observations is that different robots’ visual motions have similar patterns when they execute similar skills (e.g., pick up an object), as shown in Fig. III. Therefore, we leverage optical flow as an embodiment-agnostic action representation for WM’s pretraining.

We precompute optical flow for each episode in the pretraining dataset. A Convolution Neural Network (CNN) with a Multi-Layer Perceptron (MLP) is used to encode the optical flow and project the encoding to a vector with a small dimension (e.g., a 7-dimensional vector). During pretraining, this encoder is optimized with the WM fully end-to-end. When finetuning the WM for a target embodiment, the optical flow encoder is discarded, and the WM takes raw robot actions without any extra encoding. While this does create a mismatch between latent flow representations during pretraining and robot actions during finetuning, we find the finetuning process is easily able to compensate for this.

B. Latent Policy Steering with a world model

We propose Latent Policy Steering (LPS) to improve the policy’s performance during inference. Similar to prior work [9][11], policy steering is conducted by sampling B number of candidate plans from the policy (phase 3 in Fig. 2), selecting the best action plan according to the value function, and executing the plan in open-loop. Differently, our value function is more robust to distribution shifts and also guides the policy to stay close to the dataset. The following paragraphs describe our reasoning for each design.

a) *Robustness:* A vanilla value function learns to estimate future rewards and selects the best action accordingly [36]. However, in a small dataset, successful demonstrations only cover a limited set of states, and a policy may not visit the same set of states during inference. The resulting distribution shifts will make a vanilla value function not reliable for policy steering. To make our value function robust, we train the value function on 1) states in the dataset (s_t expert states), and 2) states likely to be visited by the policy (s_t' non-expert states) that could be out of the training data distribution. The expert states are the results of unroll the

WM with the actions in the dataset (line 7, Alg. 1). The non-expert states are computed by 1) querying the policy with the current observation to predict actions (line 5, Alg. 1), and 2) unrolling the WM with predicted actions (line 7, Alg. 1).

b) Pessimism: Since we are in an offline environment, we would like to stay close to the dataset instead of deviating from it, similar to the pessimism in offline RL [14][15][16][17]. We assume that the expert and non-expert states generated from the same observation have a 1-to-1 correspondence (line 6-7, Alg. 1). Thus, the non-expert state also shares the same environmental binary rewards as its corresponding expert state. We create a penalization for non-expert states that are deviating from the expert states based on the cosine distance between them (line 8, Alg. 1). Lastly, we create a lambda return target for the value function, similar to the latest Dreamer [28], shown from lines 9-10, Alg. 1.

Algorithm 1 Value function training for LPS.

- 1: **Requires:** Robot dataset $D = [(x_{1:T}, a_{1:T}, r_{1:T})_n | n = [1, \dots, N]]$ with observations, actions, and binary
 - 2: rewards, the frozen world model \mathcal{W} and policy π .
 - 3: **Initialize:** value function \mathcal{V} , horizon h , discount γ , and λ for return computation.
 - 4: Samples $(x_{t:t+h}, a_{t:t+h}, r_{t:t+h})$ from D .
 - 5: Sample a predicted action plan: $a'_{t:t+h} \sim \pi(x_t)$.
 - 6: $s_t = \mathcal{W}_{\text{frozen}}.\text{encode}(x_t) \triangleright$ observations to latent states.
 - 7: $s_{t:t+h}, s'_{t:t+h} = \mathcal{W}_{\text{frozen}}(s_t, a_{t:t+h}), \mathcal{W}_{\text{frozen}}(s_t, a'_{t:t+h}) \triangleright$ unroll the \mathcal{W} with actions.
 - 8: $r'_{t:t+h} = r_{t:t+h} + (\text{cosine}(s_{t:t+h}, s'_{t:t+h}) - 1)/2 \triangleright$ penalize deviation from the dataset.
 - 9: $R_\lambda, R'_\lambda = \text{return}(r_{t:t+h}, \gamma, \lambda), \text{return}(r'_{t:t+h}, \gamma, \lambda)$
 - 10: $R_{\text{all}}, S_{\text{all}} \leftarrow \text{concat}(R_\lambda, R'_\lambda), \text{concat}(s_{t:t+h}, s'_{t:t+h})$
 - 11: Optimize the value function \mathcal{V} with the loss: $\mathcal{L}(R_{\text{all}}, V(S_{\text{all}}))$.
-

c) Inference with LPS: A large batch of action plans is sampled from the BC policy during inference, as shown in phase 3 of Fig. 2. We use a batch size of $b = 400$. After encoding the current observation, the WM predicts the corresponding future states for each plan and computes the state values. A value is assigned to each plan based on a weighted average of state values with a discount factor, by assigning heavier weights to future states. The motivation is to accommodate the fact that the value function is not perfect. In practice, we found that this discounted weighted averaging of values works better than using the average or the last-state value per plan to represent the plan-level value. The action plan with the highest value is executed in open loop.

C. Algorithm summary

Our approach includes 3 phases: 1) We curate a pre-training video dataset including different robots and humans completing manipulation tasks. We compute optical flow between frames as actions and pretrain a WM with optical flow as the action representation. 2) We collect a small robot dataset on the robot to learn a policy from scratch.

We finetune the WM on the robot dataset with robot action (discarding the optical flow encoder). We also learn a robust value function for LPS (Alg. 1). Lastly, 3) We improve the action selection during inference by policy steering with the robust value function. An illustration is provided in Fig. 2.

V. EXPERIMENTS

The proposed method is evaluated on object manipulation tasks from a simulated benchmark (Robomimic [37]) and real world environments. We compared our approach to baselines with a pretrained policy and learning from scratch. Ablations are provided to verify the key choices of the algorithm and the effectiveness of the embodiment-agnostic actions across a wide range of embodiments. In the following, we first describe our experiment settings, including environment, datasets, and baselines.

A. Settings

Environment: Robomimic. Our approach and baselines are evaluated on a Franka robot across 3 tasks (Lift, Can, Square) from Robomimic [37]. Instead of leveraging 300 expert demonstrations provided by the benchmark, we only use the 30-50 expert demonstrations to learn/finetune our models, mimicking a low-data regime setting. For model pretraining, we use Robosuite [38] with a joystick to collect 100 demonstrations on 3 robots other than Franka: IIWA, UR5e, and Kinova3 via the Robosuite interface. In this case, the pretraining data has action labels inherently different from those of the Franka robot. Our evaluation protocol is similar to [39]. We report the average success rates and standard deviations across 3 seeds. Each seed has a success rate based on hundreds of evaluations.

Environment: Real world. We create an evaluation environment with a Franka robot, a desk, and objects to manipulate (cups, pot, spoon, oven, towel, beads, pan, toy radish), shown in Fig. V-A. We mount a wrist camera on the robot’s wrist and a fixed camera on the side. For each task, only the objects involved in the task will be presented. The target dataset is collected via teleoperation with joystick. The positions of the objects during data collection are randomly selected from the desk area. The object positions during evaluations include 20 positions that are pre-selected, uniformly covering in the desk area. We consider five tasks, with three basic manipulation tasks (put-radish-in-pot, stack-cups, open-oven-put-pot-in-close-oven), and two challenging long-horizon tasks that require tool use or precision (scoop-beads-with-spoon, fold-towel-to-triangle). Scooping requires the robot to use a spoon to move small beads from a pan to a bowl. Imprecise manipulation will easily lead to beads falling out of the spoon. Folding requires multiple pick-and-place actions to align the towel’s corners.

Datasets. We use pretraining datasets and target datasets in our experiment. The target dataset is a small Franka dataset with robot actions (e.g., end-effector pose) and expert quality (all demonstrations succeed and result in task completions), used to learn a policy and finetune the WM. The pretrain dataset is used to pretrain the WM, without assuming expert



Fig. 4. **Real world environment.** We conduct the real-world experiment in a table-top setting with a Franka robot, given a set of common objects.

quality. It was made of data collected in simulation, existing public robot datasets, or easy-to-collect human data. In our case, we ask the human to interact with the desk environment without a specific purpose, known as data from play. We consider 3 pretraining data variants:

- -sim: A dataset of simulation robot data collected by a human teleoperator. It includes 3 robots, different from the robot used for evaluation (target robot) with 100 demonstrations for each robot.
- -real: A set of public robot data collected by different research groups in the real world (Open X-Embodiment [4]). Since most of the object manipulation data comes from several popular robots in the Open X-embodiment dataset, we filter data from 5 popular robots. The resulting dataset has 2000 episodes after dropping some short or long episodes.
- -human: A dataset made of human video data from play. A human is asked to interact with the environment without specific goals. Therefore, frequent unintentional task completions/resets throughout the playing episode contain richer information to learn, compared to an episode collected via teleoperations. It’s total transitions is about 43% of the public robot dataset.
- -mix: the mixture of robot data in simulation, real world, and human data. In total, it has 8 different embodiments, including 3 robots in simulation, 4 robots in the real world, and a human embodiment.

Baselines. Variants of our approach are denoted by *. The suffix of LPS (-sim/real/human/mix) denotes the variants of our approach, with different pretraining dataset mixtures.

- BC: a diffusion policy [2] without pretraining. It is learned via behavior cloning on the target dataset. All of our experiments use an action-chunking size of 16.
- HPT: a pretrained policy [22] finetuned on the target dataset. The transformer backbone is frozen, and the action prediction head and the low-level encoder are finetuned. It uses an action chunking size of 16.
- LPS*: our proposed method (LPS) without pretraining the WM. The WM is trained only on the target dataset. The WM will be combined with the policy (BC), and has a prediction horizon of 16. The best action plan, according to the WM, is executed in open loop.
- LPS-(sim/real/human/mix)*: LPS with WMs pretrained on robot data from simulations (-sim), public robot

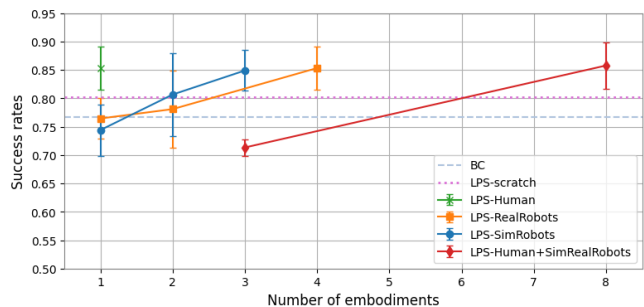


Fig. 5. **Effects of the pretrain embodiments.** World Models (WM) are pretrained on data with different embodiments (i.e., recipes). They are finetuned on the same robot dataset and combined with the same policy to solve the same task. We observe a promising trend: our approach can effectively leverage data across multiple embodiments. By increasing the number of pretraining embodiments, the amount of pretraining data grows, results in better performance compared to the policy-only baseline (BC) and WM without pretraining (i.e., LPS-scratch). Surprisingly, human video data leads to a competitive WM checkpoint (green), compared to the recipe with more embodiments and more data.

data collected in the real world (-real), human videos collected in the real world(-human), or the mixture of -sim/real/human. It has a prediction horizon of 16. The best action plan, according to the WM, is executed in open-loop

LPS* and LPS-(sim/real/human/mix)* use the same base policy as the BC baseline. Except for HPT, all policies are learned from scratch, given a small target dataset.

B. Comparisons in the simulation & real world

We compared LPS’s variants without pretraining (LPS*) and with pretraining (LPS-sim/real/human/mix*) against a behavior cloned policy (BC) across tasks both in the Robomimic and real world. LPS uses the exact same policy as the BC baseline. The main difference is that LPS uses a WM and a robust value function to select the best action from the BC.

In general, the LPS with a pretrained WM (LPS-sim/real/human/mix*) consistently improves the policy (BC) performance across tasks both in the simulation and real world (Table I, Table II). Thanks to the embodiment-agnostic action representation via optical flow, increasing the embodiments in the dataset results in a larger usable dataset. This advantage translates into better overall performance.

C. Comparisons of different embodiments for pretraining

We explore how different combinations/numbers of embodiments for pretraining affect the performance during evaluations on the Can task from Robomimic. Our target dataset has 50 demonstrations, and the pretraining dataset could include simulation-only robot data, real-world robot data, and human video data from play. The BC baseline is a behavior cloning policy, and LPS-scratch uses a WM learned from scratch to improve the BC policy. Other LPS variants use different recipes of embodiments during pretraining. We observe a promising trend: due to our embodiment-agnostic action representation that allows us to leverage cross-embodiment data, increasing the number of

TABLE I
LATENT POLICY STEERING WITH WM IN ROBOMIMIC

Task\ Setting	30 Franka demonstration					50 Franka demonstration				
	From scratch		Pretrain-and-finetune			From scratch		Pretrain-and-finetune		
	BC	LPS*	LPS -sim*	LPS -real*	LPS -mix*	BC	LPS*	LPS -sim*	LPS -real*	LPS- mix*
Lift	25.6±3.6	18.0±5.6	24.7±1.4	24.5±1.7	24.4±1.9	82.0±6.2	52.7±5.0	84.4±10.8	84.0±1.5	84.4±10.8
Can	64.9±10.2	74.7±3.1	71.1±1.0	71.5±1.7	73.1±1.5	76.7±2.1	80.2±4.9	84.9±3.6	85.3±3.8	85.8±4.1
Square	19.4±2.5	20.6±3.6	24.2±5.6	21.3±3.6	21.3±3.6	44.8±6.5	48.3±19.7	52.4±7.2	49.5±0.6	49.0±6.4
Average	36.6%	37.8%	40.0%	39.1%	39.6%	67.8%	60.0%	74.9%	72.9%	73.1%

We report the mean success rate across 3 seeds with standard deviations. The proposed method (LPS, LPS-sim*/real*/mix*) can greatly improve a policy (BC) via a WM during inference, in low-data regime. We found not only the simulation data helps to improve the performance (LPS-sim*) via WM pretraining, real-world robot and human data improves the WM via pretraining as well (LPS-real*/mix*).

TABLE II
LATENT POLICY STEERING WITH WM IN THE REAL WORLD

Task\Settings	30 ^a or 50 ^b Franka demonstrations						50 ^c or 100 ^d Franka demonstrations					
	From scratch			Pretrain-and-finetune			From scratch			Pretrain-and-finetune		
	BC	LPS*	HPT	LPS -real*	LPS -human*	LPS -mix*	BC	LPS*	HPT	LPS -real*	LPS -human*	LPS -mix*
Put-radish-in-pot	14/20 _a	15/20 _a	5/20 _a	16/20 _a	17/20_a	\	16/20 _c	18/20 _c	10/20 _c	20/20_c	20/20_c	\
Stack-cups	10/20 _a	14/20 _a	2/20 _a	14/20 _a	16/20_a	\	14/20 _c	14/20 _c	3/20 _c	15/20 _c	17/20_c	\
Open-oven-put-pot-in-close-oven	2/20 _a	6/20 _a	0/20 _a	9/20_a	8/20 _a	\	8/20 _c	11/20 _c	0/20 _c	12/20_c	11/20 _c	\
Average	43.3%	58.3%	11.7%	65.0%	68.3%	\	63.3%	71.7%	21.7%	78.3%	80.0%	\
Scoop-beads-with-spoon	6/20 _b	5/20 _b	0/20 _b	\	\	10/20_b	13/20 _d	16/20_d	0/20 _d	\	\	16/20_d
Fold-towel-to-triangle	0/20 _b	0/20 _b	0/20 _b	\	\	2/20_b	9/20 _d	11/20 _d	3/20 _d	\	\	13/20_d
Average	15.0%	12.5%	0.0%	\	\	30.0%	55.0%	67.5%	7.5%	\	\	72.5%

We report the number of successes out of 20 trials in the real world. Given challenging tasks with limited data, our method improves a policy (BC) during inference via a WM (LPS*, LPS-real*/human*/mix*). Specifically, pretraining the WM on different embodiments (LPS-real*/human*/mix*) leads to better results than the WM learned from scratch (LPS*).

embodiments leads to more usable data and results in better performance compared to the policy-only baseline (bc) and WM without pretraining.

Surprisingly, we observe that the human video data from play leads to a very competitive pretrained WM, despite having less data compared to other data mixtures with more embodiments. We suspect that this benefit comes from the human demonstrator, who can demonstrate more diverse and coherent manipulation skills in a shorter time with their hands compared to a teleoperation device. The resulting data are of higher quality compared to the teleoperation data, which are used to collect most of the large robot datasets.

D. Comparing optical flow to EEF actions

Robot end-effector pose (EEF) is another potentially embodiment-agnostic action representation for manipulators. In simulation, we investigate the advantage of using optical flow as an action representation during pretraining over EEF pose, given a pretraining dataset with 3 different robots. Our approach (LPS-sim(flow)*) uses optical flow action during pretraining, and LPS-sim(eef) uses EEF action during pretraining. Both are finetuned on the target dataset with 30 or 50 demonstrations, using the EEF robot action.

The results are shown in Table III. The advantage of optical flow as embodiment-agnostic actions vs. EEF actions

TABLE III
WMS PRETRAIN WITH OPTICAL FLOW VS. EEF ACTIONS

Task\Settings	30 demonstrations		50 demonstrations	
	LPS-sim (flow)*	LPS-sim (eef)	LPS-sim (flow)*	LPS-sim (eef)
Lift	24.7±1.4	24.6±2.0	84.4±10.8	81.9±8.7
Can	71.1±1.0	73.7±17	84.9±3.6	84.4±7.2
Square	24.2±5.6	21.0±16	52.4±7.2	45.3±21
Average	40.0%	39.8%	73.9%	70.5%

We compare the WM pretrained with embodiment-agnostic actions (optical flow) against the WM pretrained with end-effector action (eef). On a dataset of 3 robots, the optical-flow-based WM leads to better results. We believe the performance gap over the eef action will grow when more embodiments are provided.

is clear, given 3 embodiments. We suspect the advantage will keep growing when the dataset size is larger and the number of embodiments is larger. Notice that optical flow also allows human embodiment to be part of pretraining, while EEF actions are only available for robots

E. LPS's performance across horizons

We investigate LPS's performance with different action chunking horizons and the WM's prediction horizon from small to large. The WM's prediction horizon always matches

the action chunking size. We learn the policy and the WM from scratch, given EEF action, with 100 demonstrations on the Can task of Robomimic [37].

We found that LPS with a WM performs better than BC at horizons 4,8,16,20, and performs worse than BC for a horizon of 24 (Fig. V-C). Large action chunking size/horizon of 24 leads to suboptimal policy with poor performance, and the penalization on deviation from the dataset will be noisy (lines 8-10, Alg. 1). This results in a noisy reward and makes the value function less useful.

F. Ablations on the LPS’s robust value function

LPS uses a robust value function that has seen data that are both in-distribution and out-of-distribution, and it penalizes all behaviors deviating from the dataset, where the policy may not be recovered from. We verify these ideas via 2 variants of LPS.

- LPS-vanilla: This variant does not let the value function see the out-of-distribution data. Policy Steering with WM and vanilla value function (PS-vanilla) is a variant that learns a vanilla value function on the dataset, given environmental rewards. It will select the best candidate based on the value function.
- LPS-bootstrap: Policy Steering with bootstrapping is a variant that learns a value function both on the dataset (in-distribution), and outside of the dataset (out-of-distribution). It achieves this by simulating the states likely visited by the policy and learns a value function. Different from LPS, the extra states are labeled with the same rewards as the dataset’s states and do not include the term penalizing deviation from the expert states ($r'_{t:t+h} = r_{t:t+h}$ at line 8, 1). It will select the best candidate based on the value function.

All the models use 100 demonstrations to train from scratch, and no pretraining are involved.

The result shown in Table IV demonstrates that all the designs of the value function contribute to the success of LPS. A vanilla LPS has never seen out-of-distribution data. Thus, it is not robust to the distribution shift during inference. Despite seeing out-of-distribution data, LPS-bootstrap treats it optimistically and does not penalize behavior that deviates

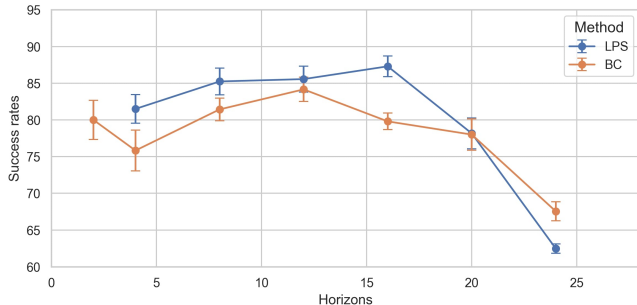


Fig. 6. **Latent Policy Steering with different horizons.** We found the proposed LPS method can effectively improve policy performance from a shorter horizon to a longer horizon up to 16. When the horizon becomes very long (e.g., 20, 24), the reward based on state similarity becomes noisy, making the value function less useful during inference.

TABLE IV

LATENT POLICY STEERING WITH ABLATIONS ON THE VALUE FUNCTION

Task \ Settings	BC	LPS-vanilla	LPS-bootstrap	LPS
Lift	99.1±0.4	96.0±4.1	98.7±0.3	99.3 ±0.9
Can	79.8±1.6	82.2±4.8	80.2±4.3	87.3±3.9
Square	45.6±1.1	52.0±7.1	48.5±18.8	52.9±9.8
Transport	30.4±32.9	20.4±1.4	22.0±2.1	34.6±21.6
Average	63.7%	62.6%	62.3%	68.5%

We ablate our designs of the robust value function for LPS into 2 variants (LPS-vanilla/bootstrap). In both variants, performance is lower than the policy-only baseline (BC), demonstrating the necessity of designing the robust value function to let WM benefit the policy (BC).

from the training dataset. Both variants perform worse than a simple policy-only baseline (BC). This shows that a robust value that has seen in/out-of-distribution data and penalizes deviation from the dataset is crucial to make a WM helpful for policy inference.

VI. CONCLUSION

We pretrain an embodiment-agnostic World Model (WM) on existing or cost-effective data sources such as public multi-embodiment robot datasets [4], robot data from simulations [38], and easily collected human data from play to improve visuomotor policies with a small amount of real-world data. Thanks to the optic flow as an embodiment-agnostic action representation, the pretrained WM has minimal dependency on specific embodiments and can be easily finetuned to a target embodiment for deployment with a small amount of data. Through 5 real-world tasks, our proposed method improves a policy’s relative performance during inference over 50% with 30-50 expert demonstrations, and over 25% relative improvement with expert 50-100 demonstrations, showing its effectiveness over prior work without pretraining a WM. The code for pretraining and finetuning the WM for LPS will be made publicly available.

REFERENCES

- [1] A. Brohan, N. Brown, J. Carbajal, Y. Chebotar, J. Dabis, C. Finn, K. Gopalakrishnan, K. Hausman, A. Herzog, J. Hsu *et al.*, “Rt-1: Robotics transformer for real-world control at scale,” *arXiv preprint arXiv:2212.06817*, 2022.
- [2] C. Chi, Z. Xu, S. Feng, E. Cousineau, Y. Du, B. Burchfiel, R. Tedrake, and S. Song, “Diffusion policy: Visuomotor policy learning via action diffusion,” *The International Journal of Robotics Research*, p. 02783649241273668, 2023.
- [3] N. M. Shafiqullah, Z. Cui, A. A. Altanzaya, and L. Pinto, “Behavior transformers: Cloning k modes with one stone,” *Advances in neural information processing systems*, vol. 35, pp. 22955–22968, 2022.
- [4] Q. Vuong, S. Levine, H. R. Walke, K. Pertsch, A. Singh, R. Doshi, C. Xu, J. Luo, L. Tan, D. Shah *et al.*, “Open x-embodiment: Robotic learning datasets and rt-x models,” in *Towards Generalist Robots: Learning Paradigms for Scalable Skill Acquisition@ CoRL2023*, 2023.
- [5] O. M. Team, D. Ghosh, H. Walke, K. Pertsch, K. Black, O. Mees, S. Dasari, J. Hejna, T. Kreiman, C. Xu *et al.*, “Octo: An open-source generalist robot policy,” *arXiv preprint arXiv:2405.12213*, 2024.
- [6] T. Henighan, J. Kaplan, M. Katz, M. Chen, C. Hesse, J. Jackson, H. Jun, T. B. Brown, P. Dhariwal, S. Gray *et al.*, “Scaling laws for autoregressive generative modeling,” *arXiv preprint arXiv:2010.14701*, 2020.

- [7] K. Black, N. Brown, D. Driess, A. Esmail, M. Equi, C. Finn, N. Fusai, L. Groom, K. Hausman, B. Ichter *et al.*, “pi0: A vision-language-action flow model for general robot control, 2024,” URL <https://arxiv.org/abs/2410.24164>.
- [8] J. Kaplan, S. McCandlish, T. Henighan, T. B. Brown, B. Chess, R. Child, S. Gray, A. Radford, J. Wu, and D. Amodei, “Scaling laws for neural language models,” *arXiv preprint arXiv:2001.08361*, 2020.
- [9] M. Nakamoto, O. Mees, A. Kumar, and S. Levine, “Steering your generalists: Improving robotic foundation models via value guidance,” *arXiv preprint arXiv:2410.13816*, 2024.
- [10] Y. Wang, L. Wang, Y. Du, B. Sundaralingam, X. Yang, Y.-W. Chao, C. Perez-D’Arpino, D. Fox, and J. Shah, “Inference-time policy steering through human interactions,” *arXiv preprint arXiv:2411.16627*, 2024.
- [11] Y. Wu, R. Tian, G. Swamy, and A. Bajcsy, “From foresight to forethought: Vlm-in-the-loop policy steering via latent alignment,” *arXiv preprint arXiv:2502.01828*, 2025.
- [12] G. Zhou, H. Pan, Y. LeCun, and L. Pinto, “Dino-wm: World models on pre-trained visual features enable zero-shot planning,” *arXiv preprint arXiv:2411.04983*, 2024.
- [13] R. Mendonca, S. Bahl, and D. Pathak, “Structured world models from human videos,” *arXiv preprint arXiv:2308.10901*, 2023.
- [14] S. Fujimoto, D. Meger, and D. Precup, “Off-policy deep reinforcement learning without exploration,” in *International conference on machine learning*. PMLR, 2019, pp. 2052–2062.
- [15] T. Yu, G. Thomas, L. Yu, S. Ermon, J. Y. Zou, S. Levine, C. Finn, and T. Ma, “Mopo: Model-based offline policy optimization,” *Advances in Neural Information Processing Systems*, vol. 33, pp. 14 129–14 142, 2020.
- [16] R. Kidambi, A. Rajeswaran, P. Netrapalli, and T. Joachims, “Morel: Model-based offline reinforcement learning,” *Advances in neural information processing systems*, vol. 33, pp. 21 810–21 823, 2020.
- [17] A. Kumar, A. Zhou, G. Tucker, and S. Levine, “Conservative q-learning for offline reinforcement learning,” *Advances in neural information processing systems*, vol. 33, pp. 1179–1191, 2020.
- [18] S. Karamcheti, S. Nair, A. S. Chen, T. Kollar, C. Finn, D. Sadigh, and P. Liang, “Language-Driven Representation Learning for Robotics,” Feb. 2023, arXiv:2302.12766 [cs]. [Online]. Available: <http://arxiv.org/abs/2302.12766>
- [19] S. Nair, A. Rajeswaran, V. Kumar, C. Finn, and A. Gupta, “R3m: A universal visual representation for robot manipulation,” *arXiv preprint arXiv:2203.12601*, 2022.
- [20] A. Majumdar, K. Yadav, S. Arnaud, Y. J. Ma, C. Chen, S. Silwal, A. Jain, V.-P. Berges, P. Abbeel, J. Malik, D. Batra, Y. Lin, O. Maksymets, A. Rajeswaran, and F. Meier, “Where are we in the search for an Artificial Visual Cortex for Embodied Intelligence?” Feb. 2024, arXiv:2303.18240 [cs]. [Online]. Available: <http://arxiv.org/abs/2303.18240>
- [21] I. Radosavovic, T. Xiao, S. James, P. Abbeel, J. Malik, and T. Darrell, “Real-world robot learning with masked visual pre-training,” in *Conference on Robot Learning*. PMLR, 2023, pp. 416–426.
- [22] L. Wang, X. Chen, J. Zhao, and K. He, “Scaling proprioceptive-visual learning with heterogeneous pre-trained transformers,” *Advances in Neural Information Processing Systems*, vol. 37, pp. 124 420–124 450, 2024.
- [23] A. Brohan, N. Brown, J. Carbajal, Y. Chebotar, X. Chen, K. Choremanski, T. Ding, D. Driess, A. Dubey, C. Finn *et al.*, “Rt-2: Vision-language-action models transfer web knowledge to robotic control,” *arXiv preprint arXiv:2307.15818*, 2023.
- [24] M. J. Kim, K. Pertsch, S. Karamcheti, T. Xiao, A. Balakrishna, S. Nair, R. Rafailov, E. Foster, G. Lam, P. Sanketi, Q. Vuong, T. Kollar, B. Burchfiel, R. Tedrake, D. Sadigh, S. Levine, P. Liang, and C. Finn, “OpenVLA: An Open-Source Vision-Language-Action Model,” Sep. 2024, arXiv:2406.09246 [cs]. [Online]. Available: <http://arxiv.org/abs/2406.09246>
- [25] S. Bahl, A. Gupta, and D. Pathak, “Human-to-Robot Imitation in the Wild,” Jul. 2022, arXiv:2207.09450 [cs, eess]. [Online]. Available: <http://arxiv.org/abs/2207.09450>
- [26] S. Bahl, R. Mendonca, L. Chen, U. Jain, and D. Pathak, “Affordances from Human Videos as a Versatile Representation for Robotics,” Apr. 2023, arXiv:2304.08488 [cs]. [Online]. Available: <http://arxiv.org/abs/2304.08488>
- [27] D. Hafner, T. Lillicrap, I. Fischer, R. Villegas, D. Ha, H. Lee, and J. Davidson, “Learning latent dynamics for planning from pixels,” in *International conference on machine learning*. PMLR, 2019, pp. 2555–2565.
- [28] D. Hafner, J. Pasukonis, J. Ba, and T. Lillicrap, “Mastering diverse domains through world models,” *arXiv preprint arXiv:2301.04104*, 2023.
- [29] A. Y. Ng, S. Russell *et al.*, “Algorithms for inverse reinforcement learning,” in *Icml*, vol. 1, no. 2, 2000, p. 2.
- [30] B. Eisner, H. Zhang, and D. Held, “FlowBot3D: Learning 3D Articulation Flow to Manipulate Articulated Objects,” May 2024, arXiv:2205.04382 [cs]. [Online]. Available: <http://arxiv.org/abs/2205.04382>
- [31] H. Zhang, B. Eisner, and D. Held, “FlowBot++: Learning Generalized Articulated Objects Manipulation via Articulation Projection,” May 2024, arXiv:2306.12893 [cs]. [Online]. Available: <http://arxiv.org/abs/2306.12893>
- [32] C. Yuan, C. Wen, T. Zhang, and Y. Gao, “General Flow as Foundation Affordance for Scalable Robot Learning,” Sep. 2024, arXiv:2401.11439 [cs]. [Online]. Available: <http://arxiv.org/abs/2401.11439>
- [33] L.-H. Lin, Y. Cui, A. Xie, T. Hua, and D. Sadigh, “FlowRetrieval: Flow-Guided Data Retrieval for Few-Shot Imitation Learning,” Aug. 2024, arXiv:2408.16944 [cs]. [Online]. Available: <http://arxiv.org/abs/2408.16944>
- [34] A. Goyal, A. Mousavian, C. Paxton, Y.-W. Chao, B. Okorn, J. Deng, and D. Fox, “IFOR: Iterative Flow Minimization for Robotic Object Rearrangement,” Feb. 2022, arXiv:2202.00732 [cs]. [Online]. Available: <http://arxiv.org/abs/2202.00732>
- [35] M. Verghese and C. Atkeson, “Skills Made to Order: Efficient Acquisition of Robot Cooking Skills Guided by Multiple Forms of Internet Data,” Sep. 2024, arXiv:2409.15172 [cs]. [Online]. Available: <http://arxiv.org/abs/2409.15172>
- [36] A. Kumar, A. Singh, F. Ebert, M. Nakamoto, Y. Yang, C. Finn, and S. Levine, “Pre-training for robots: Offline rl enables learning new tasks from a handful of trials,” *arXiv preprint arXiv:2210.05178*, 2022.
- [37] A. Mandlekar, D. Xu, J. Wong, S. Nasiriany, C. Wang, R. Kulkarni, L. Fei-Fei, S. Savarese, Y. Zhu, and R. Martín-Martín, “What matters in learning from offline human demonstrations for robot manipulation,” in *arXiv preprint arXiv:2108.03298*, 2021.
- [38] Y. Zhu, J. Wong, A. Mandlekar, R. Martín-Martín, A. Joshi, K. Lin, S. Nasiriany, and Y. Zhu, “robosuite: A modular simulation framework and benchmark for robot learning,” in *arXiv preprint arXiv:2009.12293*, 2020.
- [39] A. Z. Ren, J. Lidard, L. L. Ankile, A. Simeonov, P. Agrawal, A. Majumdar, B. Burchfiel, H. Dai, and M. Simchowitz, “Diffusion policy optimization,” 2024. [Online]. Available: <https://arxiv.org/abs/2409.00588>